Vienna Motor Symposium 2026

47th International Vienna Motor Symposium
22 – 24 April 2026

2026-34

Evaluation of Diesel and Ethanol in a Compression Ignition Engine with Glow Plug Support

Bewertung von Diesel und Ethanol in einem Selbstzündungsmotor mit Glühkerzenunterstützung

A. Ferrarese, Tupy S.A., Joinville, Brazil; F. Silva, C. Zabeu,
Maua Institute of Technology, Brazil;
C. da Silva, J. Fagundez, M. Martins, T. Lanzanova,
Federal University of Santa Maria, Brazil

DOI: https://doi.org/10.62626/1kkn-o6kz

This paper has been presented and published on the occasion of the 47th International Vienna Motor Symposium 2026.
All papers of this symposium are published in an anthology (ISBN 978-3-9504969-5-6) and can be ordered from the Austrian Society of Automotive Engineers (ÖVK) (https://vienna-motorsymposium.com, email: info@oevk.at).

2026-34

Evaluation of Diesel and Ethanol in a Compression Ignition Engine with Glow Plug Support

F. M. F. Silva[1], C.D.R. da Silva[2], J. L. S. Fagundez[2], M. E. S. Martins[2], T.D.M. Lanzanova[2], C. B. Zabeu[1], A. Ferrarese[3]

[1] *Engines and Vehicles Division, Instituto Mauá de Tecnologia, Praça Mauá 1 – Mauá, São Caetano do Sul, SP – Brazil*

[2] *Mechanical Engineering Department, Universidade Federal de Santa Maria, Av. Roraima, 1000 – Camobi, Santa Maria, RS – Brazil*

[3] *MWM – Tupy do Brasil Ltda., Av. das Nações Unidas, 22002 – Vila Almeida, São Paulo, SP – Brazil*

Abstract

Decarbonized mobility calls for renewable fuels in existing engines as a fast track for competitive solutions, especially on commercial vehicles. The typical application of ethanol, or other synthetic alcohol fuels produced via Power-to-X pathways, such as methanol, is in spark ignition engines. There are applications with successful results, but they are limited to engines with 20 bar BMEP, which enables ethanol versions to provide the same power and torque than diesel in the same engine size. This work evaluates ethanol as a substitute for diesel in a compression-ignition platform, using thermal efficiency as the main metric. Due to its low cetane number, ethanol does not readily autoignite under compression and therefore a glow plug is used to assist ignition. Such design could even allow simple engine adaptations supporting not only new engine design, but successful and simple retrofit. The development is presented by numerical simulation and engine test studies. The operating conditions are explored in three representative operating points—one partial-load and two full-load cases at different speeds. Each point is first run on diesel and then replicated with ethanol. Injection strategy and in-cylinder thermodynamic conditions are systematically varied to establish stable combustion and map operating windows. Comparative results quantify changes in ignition delay, heat-release behaviour and efficiency trends. Particular attention is given to glow-plug-initiated ignition, kernel formation and subsequent flame development. Under optimized intake and injection settings, ethanol achieves performance comparable to diesel while preserving combustion stability.

Keywords: Ethanol combustion; Glow plug; Compression ignition; CFD simulation; Combustion analysis; Engine efficiency.

Kurzfassung

Die Dekarbonisierung der Mobilität erfordert erneuerbare Kraftstoffe für bestehende Motoren als schnellen Weg zu wettbewerbsfähigen Lösungen, insbesondere bei Nutzfahrzeugen. Ethanol oder andere synthetische Alkoholkraftstoffe, die über Power-to-X-Verfahren hergestellt werden, wie beispielsweise Methanol, werden typischerweise in Ottomotoren eingesetzt. Es gibt Anwendungen mit erfolgreichen Ergebnissen, diese sind jedoch auf Motoren mit 20 bar effektivem Mitteldruck beschränkt, wodurch Ethanolversionen bei gleicher Motorgröße die gleiche Leistung und das gleiche Drehmoment wie Diesel liefern können. In dieser Arbeit wird Ethanol als Ersatz für Diesel in einer Selbstzünder-Plattform bewertet, wobei die thermische Effizienz als Hauptkenngröße herangezogen wird. Aufgrund seiner niedrigen Cetanzahl zündet Ethanol unter Kompression nicht ohne Weiteres selbst, weshalb eine Glühkerze zur Unterstützung der Zündung verwendet wird. Ein solches Design könnte sogar einfache Motoranpassungen ermöglichen, die nicht nur neue Motorkonstruktionen, sondern auch erfolgreiche und einfache Nachrüstungen unterstützen. Die Entwicklung wird anhand von numerischen Simulationen und Motorversuchen vorgestellt. Die Betriebsbedingungen werden an drei repräsentativen Betriebspunkten untersucht – einem Teillast- und zwei Volllastpunkten bei unterschiedlichen Drehzahlen. Jeder Punkt wird zunächst mit Diesel und dann mit Ethanol durchlaufen. Die Einspritzstrategie und die thermodynamischen Bedingungen im Zylinder werden systematisch variiert, um eine stabile Verbrennung zu erreichen und Kennfeldbereiche abzubilden. Vergleichende Ergebnisse quantifizieren Veränderungen im Zündverzug, im Wärmefreisetzungsverhalten und in den Effizienztrends. Besondere Aufmerksamkeit wird der durch Glühkerzen ausgelösten Zündung, der Kernbildung und der anschließenden Flammenentwicklung gewidmet. Unter optimierten Einlass- und Einspritzbedingungen erreicht Ethanol eine mit Diesel vergleichbare Leistung bei gleichbleibender Verbrennungsstabilität.

Schlagworte: Ethanolverbrennung; Glühkerze; Kompressionszündung; CFD-Simulation; Verbrennungsanalyse; Motoreffizienz.

Nomenclature

bTDC – Before Top Dead Center
BMEP – Brake Mean Effective Pressure
BSFC – Brake Specific Fuel Consumption
BTE – Brake Thermal Efficiency
B15 – Blend of 15% v/v of biodiesel with fossil diesel
CAD –Crank Angle Degree
CA05 – Crank Angle corresponding to 5% of released heat
CA50 – Crank Angle corresponding to 50% of released heat
CA90 – Crank Angle corresponding to 90% of released heat
CI –Compression Ignition
CFD –Computation Fluid Dynamics
CO – Carbon Monoxide
COV –Coefficient of Variation
DI – Direct Injection
DOI –Duration of Injection
ECFM – Extended Coherent Flame Model
EOI –End of Injection
E96h – Hydrated Ethanol with 4% v/v water content
IMEP –Indicated Mean Effective Pressure
HCCI – Homogeneous Charge Compression Ignition
HRR –Heat Release Rate
LCF – Low Carbon Fuel
LHV – Lower Heating Value
MFR –Mass Flow Rate
NO_x – Nitriogen Oxides
RANS – Reynolds-Averaged Navier–Stokes
SI – Spark Ignition
SOI –Start of Injection
TDC – Top Dead Center
THC – Total Hydrocarbons
TKI – Tabulated Kinetic Ignition

1. Introduction

Decarbonization targets in the transportation sector have intensified the search for low-carbon energy carriers that can be deployed rapidly and at scale, especially in segments that are difficult to electrify, such as heavy-duty road transport and heavy machines for agriculture, mining or construction. Recent reviews highlight that low-carbon fuels (LCFs), including advanced biofuels and synthetic e-fuels, are key enablers to reduce greenhouse-gas emissions from internal combustion engines while complementing, rather than competing with, direct electrification [1], [2]. Heavy-duty vehicles operate under demanding duty cycles, high annual mileages and stringent availability requirements, which makes a full and rapid transition to battery-electric powertrains challenging due to limitations in energy density, vehicle mass, charging time and infrastructure deployment along freight corridors [3]. In this context, several techno-economic and sustainability analyses concur that those renewable fuels compatible with existing compression-ignition (CI) platforms offer one of the most effective near-term pathways to mitigate well-to-wheel greenhouse-gas emissions in heavy-duty fleets, while leveraging the installed engine and refueling infrastructure [1], [4], [5]. Among the available bio-derived options, ethanol emerges as a particularly attractive candidate because it can be produced at large scale from renewable feedstocks, exhibits effective life-cycle carbon performance and is already integrated into fuel supply chains in several regions, notably in USA, Latin America, and Europe [4], [6].

Despite these advantages, the inherent physicochemical properties of ethanol pose significant hurdles when applied in conventional compression-ignition (CI) engines. Its very low cetane number, elevated heat of vaporization, and slower low-temperature oxidation kinetics are widely acknowledged to increase ignition delay and reduce auto-ignition propensity [7], [8]. Moreover, when implemented in DI CI platforms even as blends or with pilot injection, ethanol often demands increased fuel delivery or adaptive in-cylinder strategies to reach comparable output and stability relative to diesel [7], [9]. As a result, numerous investigations have adopted dual-fuel or pilot-injection approaches, or substantial hardware modifications, to overcome ignition shortcomings and maintain reliable combustion in heavy-duty engine conditions [9], [10]. However, many of these studies remain constrained to moderate load regimes (≈20 bar BMEP or lower) and do not fully address the thermal-efficiency, stability and durability demands of heavy-duty CI applications [7], [8]. Therefore, to harness ethanol's favorable sustainability profile for mainstream CI operation, innovative ignition assistance strategies that preserve engine architecture and retrofit potential are required.

To extend ethanol's applicability into high-load CI regimes, novel ignition-assistance methods are required to overcome its inherent ignition deficiency and ensure stable, efficient operation under realistic engine conditions. For instance, glow-plug initiation has been shown to significantly reduce cycle-to-cycle variation and misfire events when using low-reactivity fuels in CI engines by elevating local temperatures and accelerating the formation of a flame kernel [10]. In parallel, experimental studies using ethanol in direct-injection CI configurations consistently report long ignition delays, narrow stable operation windows and the need for very high in-cylinder temperatures or cetane-improver additives [11], [12]. Although ethanol's high latent heat of vaporization and low cetane number are often cited as key limitations, recent works exploring advanced ignition strategies and in-cylinder conditions suggest that ethanol may approach diesel-like thermal efficiency under optimized conditions [8], [9]. Nonetheless, a comprehensive evaluation that compares ethanol (with ignition assistance) directly against a diesel baseline on engine dynamometer and CFD simulation over full-load conditions remains rare. The present work addresses this gap by combining detailed CFD modelling and experimental validation across representative operating points, thereby enabling mapping of stable ethanol-ignition windows and quantification of ignition delay, heat-release behavior and thermal efficiency trends relative to diesel.

The objective of the present study is therefore to evaluate the technical feasibility of substituting diesel with ethanol in a compression-ignition engine equipped with glow-plug ignition support, by combining high-fidelity CFD modelling and controlled engine dynamometer experiments under representative operating conditions. Previous experimental and numerical investigations have shown that ignition-kernel formation and early flame development are key determinants of combustion stability in low-reactivity or low-temperature combustion regimes and must be captured accurately when designing assisted-ignition strategies [13], [14]. In parallel, studies on ethanol or bioethanol use in compression-ignition engines emphasize the need to map stable operating windows across load and speed to avoid excessive ignition delay, misfire and deterioration of efficiency [15], [16]. Building upon these insights, the present work provides a direct comparison between diesel and ethanol operation with glow-plug assistance at partial- and full-load points, quantifying ignition delay, heat-release characteristics and thermal-efficiency trends. By integrating CFD-based parametric studies with experimental validation, the findings aim to identify the conditions under which ethanol can achieve diesel-like performance while maintaining combustion stability, thereby supporting both new CI engine designs and retrofit strategies for heavy-duty transport applications.

2. State of the Art

Ethanol has been extensively investigated as a fuel for internal combustion engines due to its renewable origin, high research octane number and potential to reduce lifecycle greenhouse-gas emissions when produced from sustainable feedstocks. Comprehensive reviews show that ethanol and hydrous ethanol can be applied in both spark-ignition (SI) and compression-ignition (CI) engines, either as neat fuel, in blends or in dual-fuel concepts, with significant impacts on efficiency, combustion phasing and emissions profiles [17], [18]. From a fuel-property standpoint, ethanol is characterized by a high-octane number, relatively low lower heating value and high latent heat of vaporization, features that enable higher compression ratios and knock resistance in SI engines but also impose specific challenges for mixture preparation and ignition, particularly at low temperatures [17], [19]. Recent book chapters and reviews on alcohol-fueled engines emphasize that these attributes, combined with the oxygen content of ethanol, can contribute to cleaner combustion and improved brake thermal efficiency under properly optimized conditions, reinforcing its relevance as a strategic biofuel for the transport sector [20].

Despite its favorable sustainability profile, ethanol presents fundamental limitations when applied in compression-ignition engines, mainly due to its low cetane number, high latent heat of vaporization and different low-temperature oxidation chemistry compared with diesel. Classic reviews on ethanol–diesel blends point out that ethanol's poor autoignition quality and its strong charge-cooling effect tend to increase ignition delay and can promote unstable combustion if engine calibration or hardware are not adapted [21]. Experimental investigation of ethanol–diesel blends under diesel-like conditions has confirmed that ethanol, unlike biodiesel, cannot be used as a neat fuel in conventional CI engines because of its very low autoignition propensity, leading to markedly longer ignition delays and the need for higher ambient temperature and pressure to ensure reliable ignition [22]. Similar trends are observed when bioethanol is blended into diesel: the addition of ethanol reduces cetane number, density and lower heating value, and is systematically associated with increased ignition delay, higher specific fuel consumption and reduced brake power, particularly at higher ethanol fractions [23]. Recent work on biodiesel–ethanol–diesel ternary blends in Common Rail engines further shows that, under high-load conditions, ignition delay remains longer for blends containing ethanol and that the stable operating window narrows unless injection strategies and in-cylinder conditions are carefully optimized [24]. Collectively, these studies indicate that ethanol's low reactivity and strong charge-cooling effect pose substantial challenges to CI operation, underscoring the need for ignition-assistance mechanisms such as glow-plug support.

Because ethanol exhibits inherently poor auto-ignition behavior under diesel-engine thermodynamic conditions, several studies have explored ignition-assistance strategies, particularly glow-plug support, to enable stable combustion of low-reactivity alcohol fuels. Numerical investigations have demonstrated that glow-plug-assisted combustion can substantially reduce ignition delay and stabilize flame initiation when neat methanol is used in a diesel engine, indicating the strong influence of localized high-temperature ignition sites on overall combustion phasing [25]. Experimental studies on methanol sprays under diesel-like conditions further confirm that alcohol fuels require significantly higher ambient temperatures and longer residence times to ignite compared with conventional diesel, underscoring their limited low-temperature reactivity [26]. Complementary research examining ethanol and gasoline ignition under diesel-like conditions highlights that ethanol not only suffers from extended ignition delays but also exhibits evaporation-driven cooling effects that further suppress auto-ignition tendency [27]. Studies of ethanol–diesel blends in practical engines similarly report longer ignition delays, reduced brake thermal efficiency and increased sensitivity to injection timing unless additional ignition-promoting mechanisms are employed [28]. Altogether, these findings reinforce that alcohol fuels — especially methanol and ethanol — face inherent auto-ignition challenges in CI engines, thereby motivating the investigation of glow-plug-assisted strategies capable of enabling robust and repeatable ignition.

Although several studies have demonstrated that ethanol can be operated in compression-ignition engines using strategies such as low-heat-rejection concepts and hot-surface ignition, these investigations are typically constrained to specific hardware configurations or partial-load operating regimes and do not provide a systematic mapping of engine performance relative to a diesel baseline. For instance, Karthikeyan and Srithar [8] showed that a glow-plug-assisted low-heat-rejection diesel engine fueled with ethanol can achieve competitive brake thermal efficiency, but their work focuses on the combined effect of thermal insulation and hot-surface ignition, without isolating the specific contribution of the glow plug to ignition stability and combustion phasing under conventional engine hardware and boundary conditions. In parallel, glow-plug-assisted combustion has been extensively investigated in the context of HCCI and alternative-fuel CI engines, where the glow plug is used primarily as a controllable thermal stratification device or ignition assist for gaseous fuels such as natural gas, rather than as an enabler for neat ethanol operation. Lawler *et al.* demonstrated that an actively controlled glow plug can modulate heat release and thermal stratification in a gasoline-fueled HCCI engine, highlighting its potential as a powerful actuator for combustion control rather than as a tool specifically tailored to ethanol's long ignition delay [29]. Likewise, Gogolev *et al.* investigated a direct-injected natural gas compression-ignition engine with shielded glow plug ignition assist, emphasizing the feasibility of glow-plug-based ignition for low-reactivity fuels, but without addressing liquid oxygenated fuels such as ethanol [30]. On the other hand, recent works on ethanol utilization in CI engines have concentrated mainly on diesel–biodiesel–ethanol blends or nano-modified ethanol-containing fuels, focusing on global performance and emissions rather than on detailed ignition-kernel formation and glow-plug-assisted combustion behavior [31], [32]. Consequently, there is still a clear gap regarding integrated experimental and CFD-based studies that quantify ignition delay, kernel formation, heat-release characteristics and efficiency trends for neat ethanol in a compression-ignition engine explicitly assisted by a glow plug, and that systematically compare these results against conventional diesel operation over relevant load and speed ranges.

3. Methodology

3.1 Engine and Test Setup

The test bench consisted of a four-cylinder MWM D229 diesel engine modified to incorporate a Bosch DuraSpeed glow plug (model 0250.603.026) for controlled ignition assistance. The engine was fully instrumented to enable measurements of intake, exhaust and in-cylinder pressures, temperatures, mass flow rates, engine speed, and brake torque. The main engine specifications are summarized in Table 1.

Table 1 - Main engine specifications

Bore	105 mm
Stroke	120 mm
Connection rod length	207 mm
Compression ratio	16.9
Intake valve opening	354.3 CAD bTDC
Intake valve closing	-137.3 CAD bTDC
Exhaust valve opening	145.5 CAD bTDC
Exhaust valve closing	-347.5 CAD bTDC

High-frequency intake and exhaust pressures of cylinder #1 were measured using piezoresistive transducers (AVL LP12DA), while the in-cylinder pressure was recorded with a piezoelectric transducer (AVL GH14DK) conditioned by a 4-channel amplifier (AVL microIFEM). This configuration ensured sufficient temporal resolution for detailed combustion analysis. The injector current profile of cylinder #1 was acquired using a current clamp. All four high-speed measurement channels were connected to an AVL Indimodul data acquisition module, with monitoring and control carried out through AVL IndiCom software. Crank-angle-resolved data were collected at a resolution of 0.5 crank-angle degrees (CAD) using an AVL 365C angle encoder.

Additional sensors and acquisition systems were selected to meet the required accuracy and bandwidth for engine testing and were integrated into the in-house automation platform. Intake air mass flow was measured with an ultrasonic sensor (AVL FLOWSONIX Air), whereas the fuel mass flow rate was obtained using a Coriolis flow meter (Micro Motion CMF010). Exhaust gas composition was quantified using a Fourier-transform infrared (FTIR) analyzer (AVL SESAM i60FT SII).

Parameters from the engine control unit (ECU), including injection timing, injection duration, rail pressure, and boost control variables, were monitored and adjusted when necessary using the ETAS INCA software, ensuring consistent operation across the tested conditions. The experimental setup employed in this study is illustrated in Figure 1.

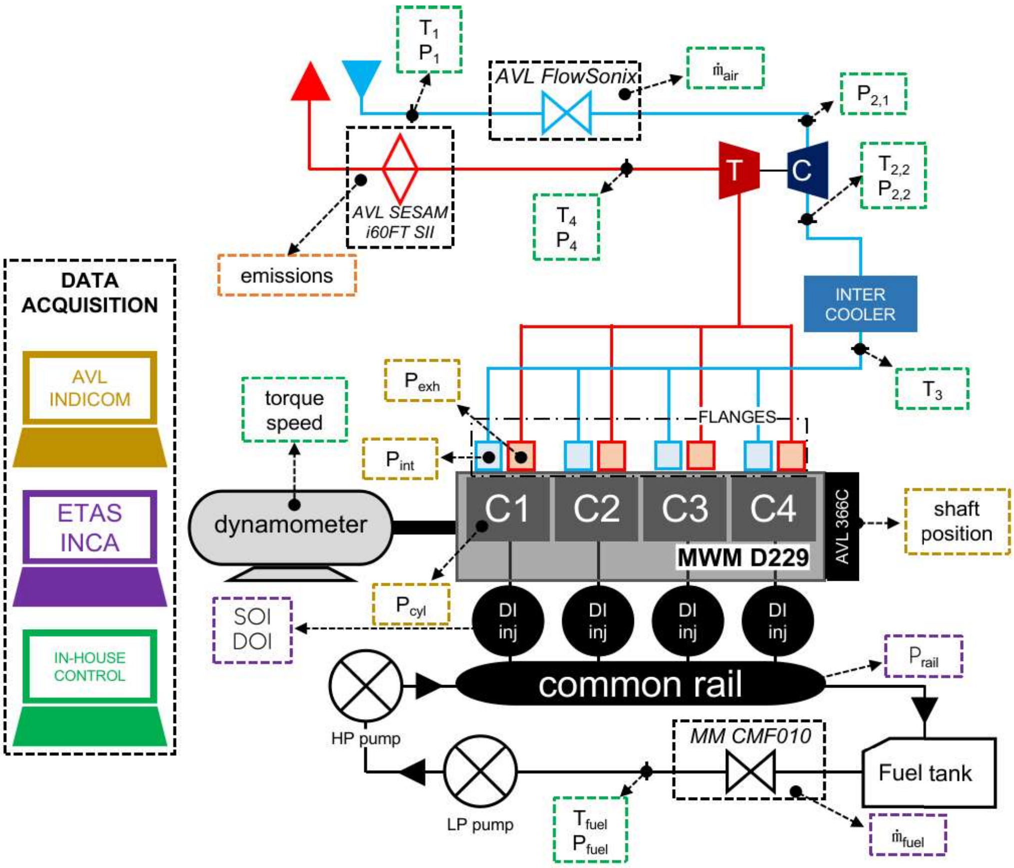

Figure 1 - Schematic view of test setup

3.2 CFD Setup

CFD simulations were conducted to provide insights into the combustion phenomena observed experimentally and to support the interpretation of the measured in-cylinder pressure and heat-release behavior. The simulations were performed using CONVERGE CFD v5.0.1 as the computational framework. Preliminary simulations carried out prior to the experimental campaign, aimed at defining the most suitable glow plug position, are outside the scope of the present study and are therefore not discussed here.

Turbulence was modeled using the Reynolds-Averaged Navier–Stokes (RANS) approach with the RNG k–ε model [33]. Combustion was described using the ECFM-3Z model [34] coupled with a Tabulated Kinetic Ignition (TKI) approach [35], generated from the C_3 Consortium chemical mechanism [36]. Within the TKI framework, the β_m parameter was systematically varied to achieve agreement between the simulated and experimentally measured in-cylinder pressure traces, ensuring an accurate reproduction of ignition delay and combustion phasing under the investigated operating condition.

The liquid fuel phase was modeled using a Lagrangian parcel-based approach. Spray atomization and breakup were described using a combination of aerodynamic and thermal breakup models in order to capture the different physical regimes governing spray evolution. Primary and secondary breakups were modeled using the Kelvin–Helmholtz and Rayleigh–Taylor (KH–RT) instability model [38], while thermally induced breakup effects associated with rapid fuel heating and spray–wall interaction were captured using the Kuhnke model [39]. This combined modeling strategy allows a consistent representation of both aerodynamically and thermal atomization, which are particularly relevant under high-temperature conditions and during glow plug–assisted ignition.

The initial droplet size distribution was described using a Rosin–Rammler function with a shape parameter of $q = 3.5$ [37]. Fuel injection was modeled according to the experimentally defined injection strategy, including the pre-injection and the main injection events. The simulations were initialized at −360 CAD and run for three consecutive engine cycles using a medium mesh to achieve cycle-to-cycle convergence. A fourth cycle was subsequently computed using a refined mesh, and only this final cycle was considered for post-processing and analysis.

Time-resolved boundary conditions were imposed for the intake and exhaust pressures based on experimental measurements. Intake and exhaust temperatures, as well as fuel mass flow rates, were prescribed using cycle-averaged values obtained from the experimental data. The computational domain is shown in Figure 2, where the inlet boundary (blue) is defined by imposed pressure, temperature, and composition, the outlet boundary (red) is defined by imposed pressure, temperature, and composition, and the glow plug surface (green) is modeled using a fixed wall temperature of 1350 °C.

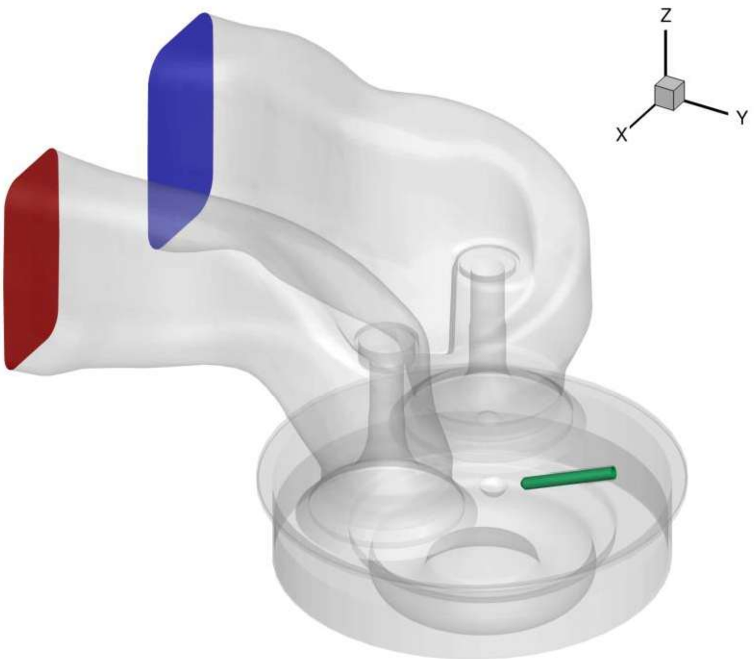

Figure 2 - Computational domain

3.3 Fuels and Operating Conditions

In this study, two fuels were investigated: diesel with a 15% v/v biodiesel blend (B15) and hydrated ethanol (E96h 4% v/v water content). The lower heating values (LHV) adopted were 41.9 MJ/kg for diesel B15 and 26.0 MJ/kg for ethanol E96h, consistent with values commonly reported in the literature. The experimental campaign was initially conducted using B15, which served as the reference fuel. The selected operating conditions were first established under diesel operation and subsequently replicated with ethanol, with the objective of maintaining equivalent brake torque levels across fuels in order to enable a consistent comparative analysis.

The operating points comprised three conditions: 1500 rpm at full load, 1500 rpm at 60% load, and 1000 rpm at full load. Numerical simulations were performed exclusively for the ethanol-fueled case at 1500 rpm and full load, allowing a more detailed investigation of the combustion and physical mechanisms associated with ethanol operation. For each operating condition, the engine was stabilized for 2 minutes, followed by a 1-minute acquisition period. The results presented correspond to time-averaged values over this measurement interval.

4. Results and Discussion

4.1 Experimental results

This section presents and discusses the experimental results obtained under the operating conditions described in the methodology. The analysis is structured to progressively relate engine performance, combustion behavior, and overall efficiency. First, global performance indicators are examined to establish a consistent basis for comparison among the tested operating points. Subsequently, gaseous emissions are evaluated to assess the environmental implications of each condition. The discussion then focuses on in-cylinder pressure traces and apparent heat release rate (HRR), providing insight into combustion characteristics and phasing. Finally, the results are consolidated through an assessment of thermal efficiency and brake-specific fuel consumption, highlighting the combined effects of combustion and operating parameters on engine performance.

4.1.1 Load Matching and Engine Operating Parameters

Table 2 summarizes the main engine operating parameters obtained at the three investigated operating points for both diesel and ethanol fueling. Although the target operating conditions were defined in the methodology section, the results presented here confirm the effectiveness of the load-matching strategy adopted in this study.

For each operating point, the ethanol tests were conducted by replicating the diesel operating conditions as closely as possible, with the engine load adjusted to achieve comparable brake torque levels. As shown in Table 2, the torque and power values obtained with ethanol are in reasonable agreement with those measured under diesel operation, with small deviations mainly associated with differences in fuel properties and combustion characteristics.

Table 2 – Main engine performance parameters measured on the test bench

n [rpm]	Load	Fuel	Torque [N.m]	Power [kW]	Exhaust λ	Air MFR [kg/h]	Fuel MFR [kg/h]
1500	100%	diesel	604.0	94.88	1.45	474.21	22.14
		ethanol	602.0	94.74	1.42	472.86	36.93
1500	60%	diesel	359.7	56.52	1.77	317.05	19.90
		ethanol	350.8	55.21	1.83	320.71	19.49
1000	100%	diesel	297.0	31.16	1.23	142.09	8.01
		ethanol	288.7	30.34	1.31	139.31	11.59

Differences in excess air ratio (λ) and mass flow rates are also observed between the two fuels. Ethanol operation generally results in higher fuel mass flow rates due to its lower heating value, while the air mass flow rates and corresponding λ values reflect the distinct mixture formation and combustion behavior of each fuel under the same nominal load condition.

These results provide the experimental basis for the subsequent analysis of gaseous emissions, in-cylinder pressure, heat-release behavior, and efficiency metrics presented in the following sections.

4.1.2 Emission Characteristics

This section presents the gaseous emission results obtained for diesel and ethanol operation at the investigated operating points with no aftertreatment system. Table 3 summarizes the brake-specific raw emissions of total hydrocarbons (THC), nitrogen oxides (NO_x), and carbon monoxide (CO), which are used to compare the emission behavior of both fuels under equivalent load conditions. Particulate matter emissions were not measured in the present study.

Table 3 – Brake-specific gaseous emissions measured at the investigated operating points

n [rpm]	Load	Fuel	THC [g/kW.h]	NO_x [g/kW.h]	CO [g/kW.h]
1500	100%	diesel	0.611	4.850	0.074
		ethanol	0.663	2.866	0.126
1500	60%	diesel	1.038	3.782	0.180
		ethanol	1.698	4.834	0.565
1000	100%	diesel	30.019	3.986	0.122
		ethanol	10.288	3.526	0.292

The results indicate a strong dependence of emission levels on both engine operating conditions and fuel properties. At 1500 rpm / full load, ethanol operation leads to a noticeable reduction in NO_x emissions compared to diesel, while THC and CO emissions remain of similar magnitude. The lower NO_x levels observed with ethanol are consistent with its lower combustion temperatures associated with charge cooling and different heat release characteristics.

At 1500 rpm / 60% load, ethanol operation results in higher THC and CO emissions relative to diesel. This behavior suggests less favorable oxidation conditions under part-load operation, likely associated with increased premixed combustion and higher sensitivity to mixture preparation. Under this condition, NO_x emissions for ethanol are slightly higher than those observed with diesel, although remaining within a comparable range.

At 1000 rpm / full load, diesel operation exhibits a pronounced increase in THC emissions, indicating incomplete oxidation at low engine speed. Under the same operating condition, ethanol operation results in significantly lower THC emissions, reflecting improved oxidation behavior despite the reduced engine speed. For this case, NO_x and CO emissions remain comparable between the two fuels.

Overall, the relatively low NO_x levels observed across all operating points are consistent with the applied combustion strategy and the temperature control achieved under the investigated conditions. These emission trends provide important context for the subsequent analysis of in-cylinder pressure and heat release behavior presented in the following section.

4.1.3 In-Cylinder Pressure and Heat Release Analysis

After establishing the load-matching conditions and the main operating parameters for all test points, the analysis is now extended to the combustion process itself. The in-cylinder pressure and the corresponding heat release rate (HRR) provide direct insight into combustion phasing, intensity, and stability for both fuels under the investigated operating conditions.

Figure 3 presents the ensemble-averaged in-cylinder pressure traces and the corresponding HRR profiles as a function of crankshaft position for diesel (B15) and ethanol (E96h), considering the three operating points analyzed.

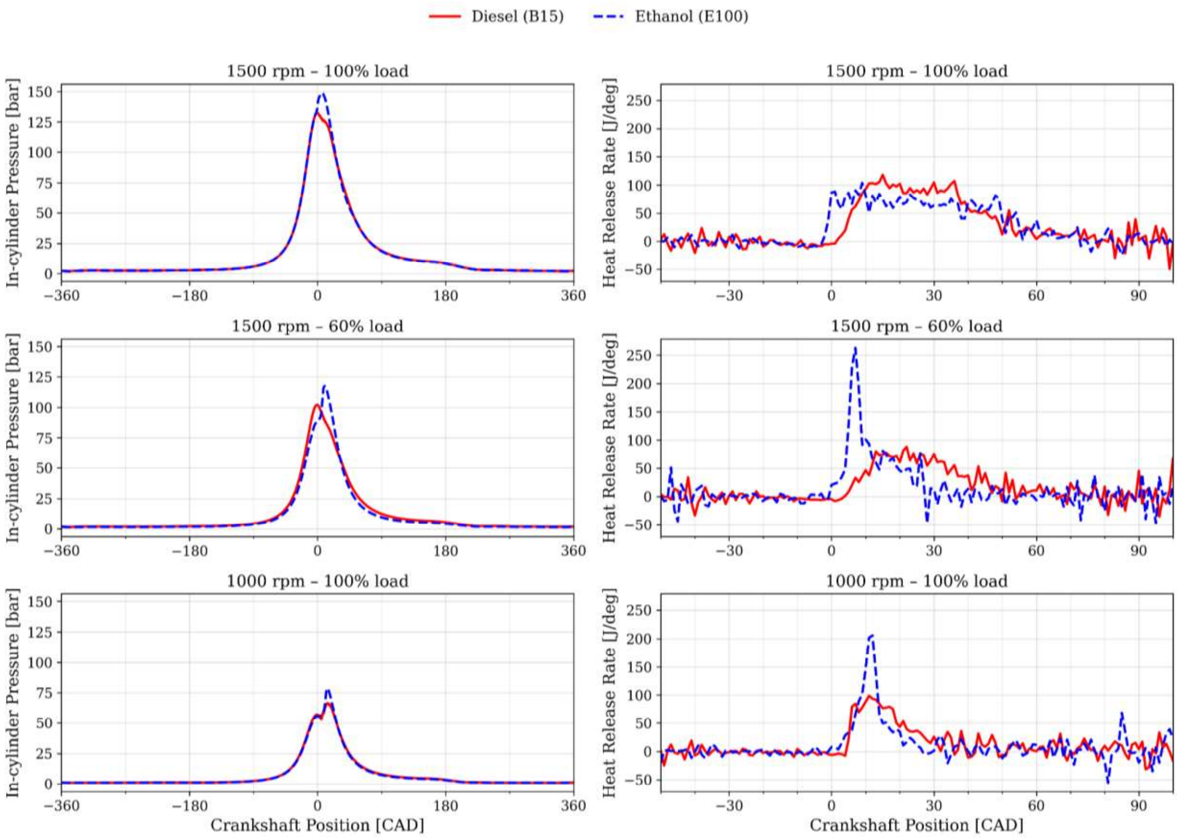

Figure 3 - In-cylinder pressure and HRR comparison

At 1000 rpm / full load, both fuels exhibit comparable peak in-cylinder pressure levels, indicating similar overall load conditions. However, ethanol shows a steeper pressure rise around top dead center (TDC), which is reflected in a higher and narrower HRR peak. This behavior indicates a more concentrated heat release close to TDC, consistent with the higher laminar flame speed and inherent oxygen content of ethanol, leading to a more rapid combustion process.

For the 1500 rpm / 60% load condition, more pronounced differences are observed in the HRR profiles. Ethanol presents a distinct and sharp premixed combustion peak with significantly higher maximum HRR, whereas diesel exhibits a smoother and more gradual heat release typical of a diffusion-controlled combustion regime. Despite these differences in combustion structure and heat release dynamics, the peak in-cylinder pressure levels remain comparable, confirming effective load matching between fuels.

At 1500 rpm / full load condition, ethanol again exhibits an earlier and more intense heat release compared to diesel, resulting in a slightly higher peak pressure. The broader HRR profile observed for diesel suggests a larger contribution from diffusion-controlled combustion, while ethanol combustion remains predominantly premixed under this operating condition. The earlier phasing of ethanol combustion is clearly reflected in the HRR onset and peak location relative to TDC.

Overall, although similar global operating conditions were achieved, the results demonstrate that the combustion dynamics differ significantly between fuels, particularly in terms of heat release rate, combustion phasing, and the balance between premixed and diffusion-controlled combustion modes.

While the ensemble-averaged in-cylinder pressure and HRR profiles provide qualitative insight into combustion behavior, a quantitative evaluation of combustion performance and stability requires cycle-resolved metrics. In this context, the indicated mean effective pressure (IMEP) represents the net indicated work per cycle, while the coefficient of variation of IMEP (COV_IMEP) is widely used as an indicator of cycle-to-cycle combustion stability. Table 4 summarizes the mean IMEP values and the corresponding COV_IMEP for diesel (B15) and ethanol (E96h) at the three operating points investigated, together with key combustion phasing metrics (CA05, CA50, and CA90).

Table 4 – IMEP, combustion stability, and combustion phasing comparison

n [rpm]	Load	Fuel	IMEP [bar]	COV_IMEP [%]	CA05 [CAD]	CA50 [CAD]	CA90 [CAD]
1500	100%	diesel	18.8	0.57	8.9	27.7	55.0
		ethanol	18.8	0.56	2.5	26.8	52.7
1500	60%	diesel	11.4	0.71	11.5	27.3	57.4
		ethanol	11.6	1.05	4.2	10.2	39.7
1000	100%	diesel	9.2	1.87	7.3	17.2	64.6
		ethanol	9.2	1.25	6.2	12.6	64.3

At 1500 rpm / full load condition, both fuels achieve essentially identical IMEP values, confirming successful load matching. Ethanol presents a slightly lower COV_IMEP, indicating marginally improved combustion stability under this high-load condition. This behavior is consistent with the earlier combustion phasing and more intense heat release observed in Figure 3.

For the 1500 rpm / 60% load condition, diesel exhibits slightly lower COV_IMEP compared to ethanol, indicating a more stable combustion process at part load. The increased cycle-to-cycle variability observed for ethanol can be attributed to its stronger premixed combustion behavior, which is more sensitive to mixture preparation and ignition conditions, as evidenced by the sharp HRR peak and the earlier CA05 and CA50 values.

At 1000 rpm / full load, both fuels again present identical IMEP values; however, ethanol shows a noticeably lower COV_IMEP compared to diesel. This result indicates improved combustion repeatability for ethanol under low-speed, high-load operation, which aligns with the more concentrated heat release around TDC observed in the HRR profile.

Overall, the IMEP and COV_IMEP results reinforce the trends identified in the pressure and HRR analyses. Ethanol operation promotes faster and earlier heat release, which can lead to improved combustion stability under high-load conditions. Conversely, under part-load operation, diesel maintains a more robust combustion behavior with lower sensitivity to cycle-to-cycle variations.

It is important to mention that operation with B15 was carried out with original engine calibration, while operation with E96h was conducted with a not fully optimized injection strategy.

4.1.4 Thermal Efficiency and Specific Fuel Consumption

Table 5 summarizes the brake specific fuel consumption (BSFC) and the corresponding brake thermal efficiency (BTE) for all operating points investigated, considering both diesel (B15) and ethanol (E96h) operation. The values were calculated from the averaged experimental data, with brake thermal efficiency derived from the measured BSFC and the adopted lower heating values of each fuel. This comparison enables a direct assessment of the influence of fuel properties and operating conditions on engine efficiency under matched load conditions.

Table 5 – BSFC and BTE comparison

n [rpm]	Load	Fuel	BSFC [g/kWh]	η_{th} [%]
1500	100%	diesel	233.38	36.8
		ethanol	389.82	35.5
1500	60%	diesel	234.78	36.6
		ethanol	352.07	39.3
1000	100%	diesel	257.00	33.4
		ethanol	382.00	36.2

At 1500 rpm / full load condition, both fuels exhibit comparable brake thermal efficiencies, despite the substantially higher BSFC observed for ethanol. This behavior is primarily attributed to the lower heating value of ethanol, which requires a higher fuel mass flow rate to deliver the same brake power. The similarity in BTE indicates that, under this condition, both fuels achieve a comparable conversion efficiency of chemical energy into mechanical work.

At 1500 rpm / 60% load condition, ethanol operation results in a noticeably higher brake thermal efficiency compared to diesel, despite its higher BSFC. This improvement suggests a more effective energy conversion process under part-load conditions when operating with ethanol. Such behavior may be associated with differences in combustion phasing, enhanced charge cooling effects, and potentially reduced heat losses, as indicated by the combustion analysis presented earlier.

At 1000 rpm / full load condition, ethanol exhibits a higher brake thermal efficiency than diesel, even though its BSFC remains significantly higher. This result indicates that, under low-speed and high-load operation, ethanol combustion allows a more favorable utilization of the supplied chemical energy, consistent with the more concentrated heat release near TDC observed in the pressure and HRR analyses.

Overall, the results highlight that although ethanol operation inherently leads to higher BSFC values due to its lower heating value, comparable or even superior brake thermal efficiencies can be achieved depending on the engine operating condition. These findings emphasize the importance of jointly analyzing BSFC and brake thermal efficiency when evaluating alternative fuels, as BSFC alone may not fully reflect the underlying energy conversion efficiency.

4.2 CFD results

This section presents the main insights obtained from the CFD simulations, with particular emphasis on the ignition process and early combustion development under ethanol operation. The numerical analysis focuses on the role of the pilot injection and its interaction with the glow plug, which governs the formation of the initial combustion kernel and subsequently controls the ignition of the main injection.

Figures 4 and 5 present a sequence of instantaneous CFD fields illustrating the temporal evolution of combustion kernel formation during the pre-injection phase. The left-hand side shows the equivalence ratio (λ) contours, while the right-hand side displays chemical source term isosurfaces, highlighting regions of active chemical reactions. Fuel spray parcels are also shown in green.

The results are presented at selected crank angle positions before top dead center (bTDC), enabling a detailed visualization of the ignition sequence and the early development of the flame kernel.

Shortly after the start of the pre-injection, a small fraction of the injected ethanol spray reaches the vicinity of the glow plug. As indicated by the λ-fields at earlier crank angles (12–10 CAD bTDC), localized mixture enrichment occurs near the glow plug surface. Due to the elevated wall temperature, this impinging fuel undergoes rapid vaporization and mixing, creating favorable thermo-chemical conditions for ignition. Autoignition is then initiated in a confined region close to the glow plug, leading to the formation of a stable combustion kernel (highlighted region).

As the crank angle advances toward TDC (8–6 CAD bTDC), the ignition kernel grows and propagates into the surrounding mixture. The chemical source term isosurfaces clearly show an expanding and highly reactive region, while the kernel remains anchored near the glow plug. This anchoring behavior ensures ignition robustness and repeatability and is facilitated by ethanol's high laminar flame speed and intrinsic oxygen content, which promote rapid flame development once ignition is triggered.

When the main injection event starts (4–2 CAD bTDC), the injected fuel enters an already reactive and high-temperature environment. As shown in the later frames of Figure 5, the fuel from the main injection ignites almost immediately upon interacting with the established combustion kernel. This interaction effectively suppresses the ignition delay of the main injection and leads to a rapid and spatially distributed combustion onset, favoring a premixed-dominated combustion regime.

Overall, the CFD results provide a clear physical interpretation of the experimental observations. The pilot injection plays a critical role in establishing a robust and well-positioned ignition kernel, while the glow plug ensures reliable ignition under ethanol operation. The interaction between the pre-injection-induced kernel and the main injection explains the earlier combustion phasing and the higher heat release rates observed in the experimental in-cylinder pressure and HRR analyses. These findings highlight the importance of injection strategy and ignition assistance in enabling stable, efficient, and controllable ethanol combustion in compression ignition engines.

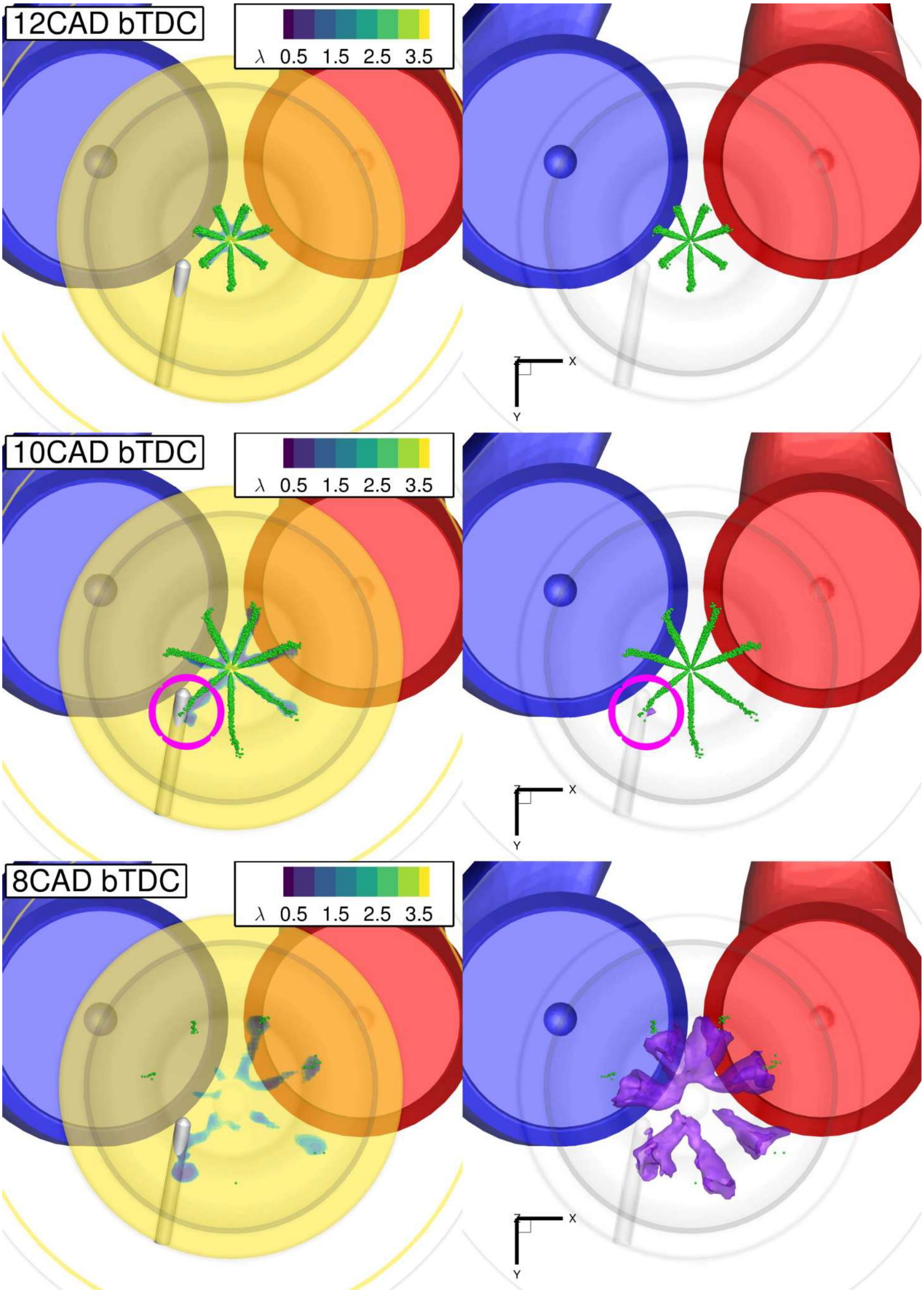

Figure 4 - CFD-predicted ignition kernel formation during pilot injection under ethanol operation (12-10 CAD bTDC)

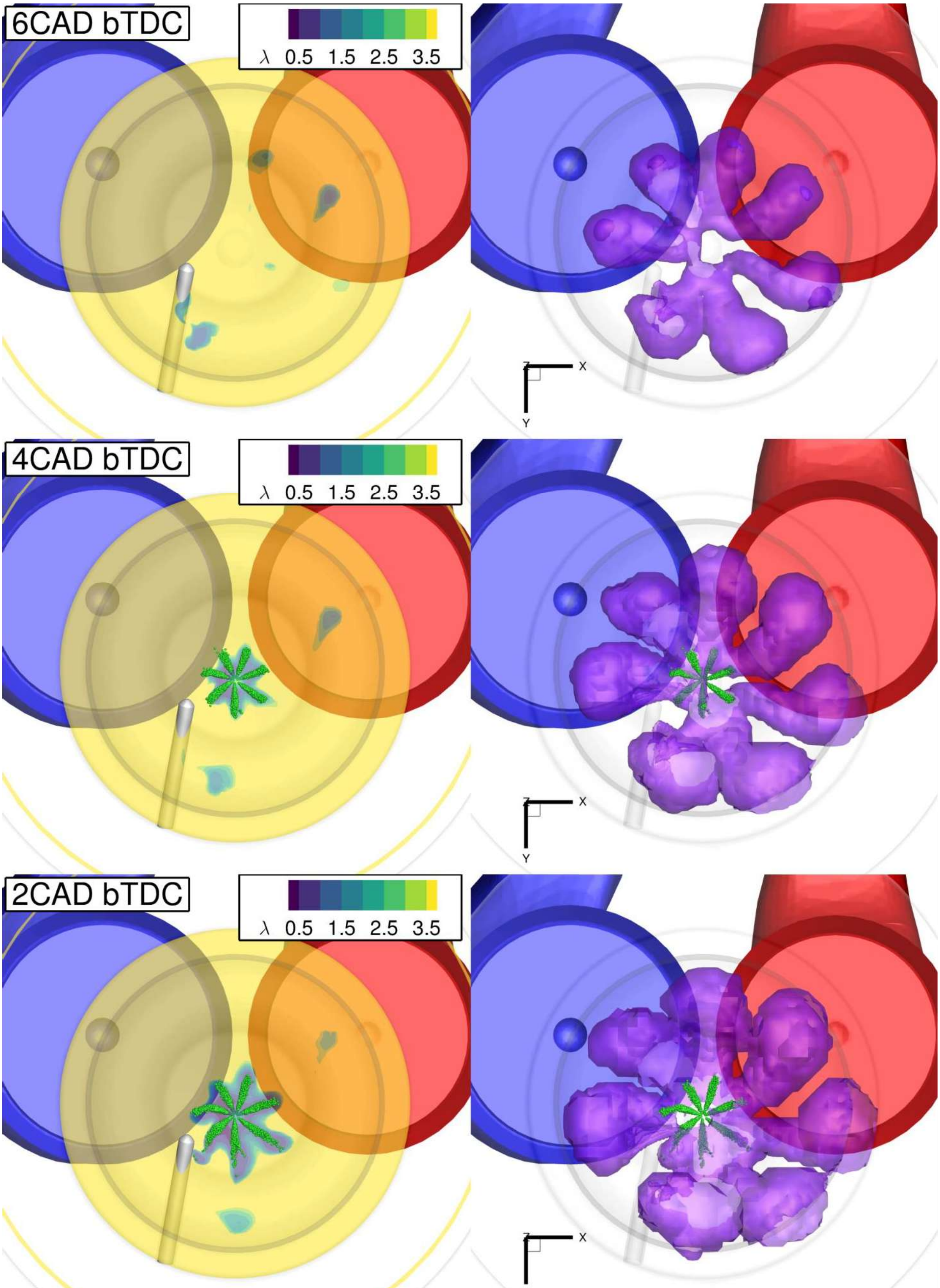

Figure 5 - CFD-predicted ignition kernel formation during pilot injection under ethanol operation (6-2 CAD bTDC)

5. Conclusions

This study investigated the combustion behavior of hydrous ethanol in a compression ignition engine with glow plug assistance, combining experimental measurements and three-dimensional CFD simulations. The results demonstrate that stable and efficient ethanol combustion can be achieved through an appropriate injection strategy coupled with thermal ignition support.

Experimental results showed that ethanol operation leads to combustion characteristics comparable to diesel under the investigated conditions, with competitive thermal efficiency and distinct emission trends. In particular, NO_x emissions were generally lower or comparable to diesel at full-load conditions, while THC and CO levels reflected the increased sensitivity of ethanol combustion to mixture preparation and ignition control. Particulate matter emissions were not measured in the present study.

The CFD analysis provided more information about ignition and early combustion processes. The simulations revealed that the pre-injection plays a fundamental role in establishing a stable ignition kernel through localized fuel–glow plug interaction. The elevated glow plug temperature promotes rapid vaporization and autoignition of a small fraction of the injected ethanol, leading to the formation of a persistent flame kernel. This kernel remains anchored near the glow plug and serves as an effective ignition source for the subsequent main injection, significantly reducing ignition delay and promoting a more controlled and premixed-dominated combustion process. The numerical findings are fully consistent with the experimentally observed pressure and heat release rate trends.

Beyond ethanol, the identified combustion mechanism is not fuel-specific and can be extended to other low-reactivity, oxygenated fuels. In this context, methanol emerges as a particularly promising candidate. Methanol can be produced from renewable pathways, including hydrogen-based synthesis routes, and shares several combustion-relevant properties with ethanol, such as high latent heat of vaporization and low cetane number. The results presented in this work suggest that glow plug-assisted ignition combined with split injection strategies could provide a viable pathway for enabling methanol combustion in compression ignition engines, potentially extending the applicability of this concept to future hydrogen-derived e-fuels.

Overall, the findings highlight the importance of coordinated injection strategy and ignition assistance in enabling low-carbon fuels in compression ignition engines. The combined experimental–numerical approach adopted in this study provides a robust framework for the development and optimization of advanced combustion concepts targeting high efficiency and reduced environmental impact.

Acknowledgments

The authors gratefully acknowledge MWM Tupy and Raízen for the support that made this research possible. Their funding and continued collaboration were essential for the development and execution of this study. This research was also supported by São Paulo Research Foundation (FAPESP), through the EMU grant #21/00759-3 and #24/21800-0. Convergent Science provided CONVERGE licenses and technical support for this work.

References

[1] J. Benajes, A. García, J. Monsalve-Serrano, and M. Guzmán-Mendoza, "A review on low carbon fuels for road vehicles: The good, the bad and the energy potential for the transport sector," *Fuel*, vol. 361, p. 130647, Apr. 2024, doi: 10.1016/J.FUEL.2023.130647.

[2] A. K. Agarwal *et al.*, "Future of internal combustion engines using sustainable, scalable, and storable E-fuels and biofuels for decarbonizing transport and enabling advanced combustion technologies," *Prog Energy Combust Sci*, vol. 110, p. 101236, Sep. 2025, doi: 10.1016/J.PECS.2025.101236.

[3] S. Mojtaba Lajevardi, J. Axsen, and C. Crawford, "Comparing alternative heavy-duty drivetrains based on GHG emissions, ownership and abatement costs: Simulations of freight routes in British Columbia," *Transp Res D Transp Environ*, vol. 76, pp. 19–55, Nov. 2019, doi: 10.1016/J.TRD.2019.08.031.

[4] T. Verger, U. Azimov, and O. Adeniyi, "Biomass-based fuel blends as an alternative for the future heavy-duty transport: A review," *Renewable and Sustainable Energy Reviews*, vol. 161, p. 112391, Jun. 2022, doi: 10.1016/J.RSER.2022.112391.

[5] A. García, J. Monsalve-Serrano, D. Villalta, and M. Guzmán-Mendoza, "Parametric assessment of the effect of oxygenated low carbon fuels in a light-duty compression ignition engine," *Fuel Processing Technology*, vol. 229, p. 107199, May 2022, doi: 10.1016/J.FUPROC.2022.107199.

[6] M. G. da Costa, D. N. S. Gonçalves, and M. de A. D'Agosto, "From commodities to high-value exports: biofuels as a catalyst for Brazil's energy transition and economic transformation," *Sustainable Energy Technologies and Assessments*, vol. 81, p. 104416, Sep. 2025, doi: 10.1016/J.SETA.2025.104416.

[7] S. Sureshchandra Bhurat, S. Ranjit Pasupuleti, R. Kunwer, S. Kumar Gugulothu, and S. Kumar Joshi, "Effect of ethanol-diesel blend on compression ignition engine: A mini review," *Mater Today Proc*, vol. 69, pp. 459–462, Jan. 2022, doi: 10.1016/J.MATPR.2022.09.139.

[8] B. Karthikeyan and K. Srithar, "Performance characteristics of a glowplug assisted low heat rejection diesel engine using ethanol," *Appl Energy*, vol. 88, no. 1, pp. 323–329, Jan. 2011, doi: 10.1016/J.APENERGY.2010.07.011.

[9] S. Lee, D. L. Pintor, and S. Cho, "Enabling ethanol mixing-controlled compression-ignition combustion using 2-Ethylhexyl nitrate in an off-road engine," *Appl Energy*, vol. 377, p. 124445, Jan. 2025, doi: 10.1016/J.APENERGY.2024.124445.

[10] C. Yao, T. Zhou, F. Yang, Y. Hu, J. Wang, and M. Ouyang, "Experimental study of glow plug assisted compression ignition," *Fuel*, vol. 197, pp. 111–120, Jun. 2017, doi: 10.1016/J.FUEL.2017.02.008.

[11] H. O. Hardenberg and A. J. Schaefer, "The use of ethanol as a fuel for compression ignition engines," *SAE Technical Papers*, 1981, doi: 10.4271/811211.

[12] J. A. John, N. Mohammed Shahinsha, K. Singh, and R. Pant, "Review on exhaust emissions of CI engine using ethanol as an alternative fuel," *Mater Today Proc*, vol. 69, pp. 286–290, Jan. 2022, doi: 10.1016/J.MATPR.2022.08.536.

[13] H. Reddy and J. Abraham, "Ignition kernel development studies relevant to lean-burn natural-gas engines," *Fuel*, vol. 89, no. 11, pp. 3262–3271, Nov. 2010, doi: 10.1016/J.FUEL.2010.05.040.

[14] Y. Wang, W. Han, T. Zirwes, F. Zhang, H. Bockhorn, and Z. Chen, "Effects of low-temperature chemical reactions on ignition kernel development and flame propagation in a DME-air mixing layer," *Proceedings of the Combustion Institute*, vol. 39, no. 2, pp. 1515–1524, Jan. 2023, doi: 10.1016/J.PROCI.2022.07.024.

[15] M. Odziemkowska, A. Matuszewska, and J. Czarnocka, “Diesel oil with bioethanol as a fuel for compression-ignition engines,” *Appl Energy*, vol. 184, pp. 1264–1272, Dec. 2016, doi: 10.1016/J.APENERGY.2016.07.069.
[16] J. S. Rosa, M. E. S. Martins, G. D. Telli, C. R. Altafini, P. R. Wander, and L. A. O. Rocha, “Exploring the effects of diesel start of injection and water-in-ethanol concentration on a reactivity controlled compression ignition engine,” *Fuel*, vol. 281, p. 118751, Dec. 2020, doi: 10.1016/J.FUEL.2020.118751.
[17] X. Wang *et al.*, “Evaluation of hydrous ethanol as a fuel for internal combustion engines: A review,” *Renew Energy*, vol. 194, pp. 504–525, Jul. 2022, doi: 10.1016/J.RENENE.2022.05.132.
[18] M. B. Mobin Siddique *et al.*, “A comprehensive review on the application of bioethanol/biodiesel in direct injection engines and consequential environmental impact,” *Clean Eng Technol*, vol. 3, p. 100092, Jul. 2021, doi: 10.1016/J.CLET.2021.100092.
[19] Ş. , A. M. Ş. , & İ. K. Altun, “Monohydric aliphatic alcohols as liquid fuels for using in internal combustion engines: A review.,” *Proceedings of the Institution of Mechanical Engineers, Part E: Journal of Process Mechanical Engineering*, 2024.
[20] S. K. Pathak, P. O. Sharma, and H. M. Singh, “Alcohol for Fueling IC Engines,” *Energy, Environment, and Sustainability*, vol. Part F1036, pp. 249–276, 2026, doi: 10.1007/978-981-96-7384-1_9.
[21] A. C. Hansen, Q. Zhang, and P. W. L. Lyne, “Ethanol–diesel fuel blends — a review,” *Bioresour Technol*, vol. 96, no. 3, pp. 277–285, Feb. 2005, doi: 10.1016/J.BIORTECH.2004.04.007.
[22] H. Kuszewski, “Experimental investigation of the autoignition properties of ethanol–biodiesel fuel blends,” *Fuel*, vol. 235, pp. 1301–1308, Jan. 2019, doi: 10.1016/J.FUEL.2018.08.146.
[23] M. Çelik, İ. Örs, C. Bayindirli, and M. Demiralp, “Experimental investigation of impact of addition of bioethanol in different biodiesels, on performance, combustion and emission characteristics,” *Journal of Mechanical Science and Technology 2017 31:11*, vol. 31, no. 11, pp. 5581–5592, Nov. 2017, doi: 10.1007/S12206-017-1052-X.
[24] N. N. Van *et al.*, “An analysis of effects of biodiesel-ethanol-diesel blended in compressed ignition engine,” *Pet Sci Technol*, 2025, doi: 10.1080/10916466.2025.2466856.
[25] R. A. Krishnan, K. Panda, and A. Ramesh, “Simulation Studies on Glow Plug Assisted Neat Methanol Combustion in a Diesel Engine,” *SAE Technical Papers*, 2022, doi: 10.4271/2022-01-0519.
[26] C. Yao, T. Zhou, F. Yang, Y. Hu, J. Wang, and M. Ouyang, “Experimental study of glow plug assisted compression ignition,” *Fuel*, vol. 197, pp. 111–120, Jun. 2017, doi: 10.1016/J.FUEL.2017.02.008.
[27] L. Starck, B. Lecointe, L. Forti, and N. Jeuland, “Impact of fuel characteristics on HCCI combustion: Performances and emissions,” *Fuel*, vol. 89, no. 10, pp. 3069–3077, Oct. 2010, doi: 10.1016/J.FUEL.2010.05.028.
[28] Y. Zhang *et al.*, “Experimental investigation of wall-film characteristics of methanol and ethanol sprays under varying flash-boiling intensities,” *Energy*, p. 139286, Nov. 2025, doi: 10.1016/J.ENERGY.2025.139286.
[29] B. Lawler, J. Lacey, O. Güralp, P. Najt, and Z. Filipi, “HCCI combustion with an actively controlled glow plug: The effects on heat release, thermal stratification, efficiency, and emissions,” Appl Energy, vol. 211, pp. 809–819, Feb. 2018, doi: 10.1016/J.APENERGY.2017.11.089.
[30] I. M. Gogolev and J. S. Wallace, “Performance and emissions of a compression-ignition direct-injected natural gas engine with shielded glow plug ignition assist,” Energy Convers Manag, vol. 164, pp. 70–82, May 2018, doi: 10.1016/J.ENCONMAN.2018.02.071.

[31] M. Dabi and U. K. Saha, “Performance, combustion and emissions analyses of a single-cylinder stationary compression ignition engine powered by Mesua Ferrea Linn oil-ethanol-diesel blend,” Clean Eng Technol, vol. 8, p. 100458, Jun. 2022, doi: 10.1016/J.CLET.2022.100458.
[32] A. Munimathan, S. Rajendran, and K. Raju, “Exhaust gas recirculation in a compression-ignition engine with nano coated Al2O3-TiO2 and ethanol fuel,” Results in Engineering, vol. 20, p. 101414, Dec. 2023, doi: 10.1016/J.RINENG.2023.101414.
[33] V. Yakhot and S. A. Orszag, Renormalization group analysis of turbulence, Journal of Scientific Computing, 1(1), pp. 3–51, 1986.
[34] O. Colin and A. Benkenida, The 3-Zone Extended Coherent Flame Model (ECFM3Z) for computing premixed/diffusion combustion, Combustion and Flame, 124(1–2), pp. 134–157, 2001.
[35] S. Angelberger et al., A tabulated autoignition model for internal combustion engine simulations, SAE Technical Paper 2003-01-1846, 2003.
[36] C_3 Consortium, C_3 chemical kinetic mechanisms for engine combustion simulations, Available through the C_3 Consortium database / publications.
[37] P. Rosin and E. Rammler, The laws governing the fineness of powdered coal, Journal of the Institute of Fuel, 7, pp. 29–36, 1933.
[38] R. D. Reitz and R. Diwakar, Structure of high-pressure fuel sprays, SAE Technical Paper 870598, 1987.
[39] D. Kuhnke, Spray/Wall Interaction Modelling by Dimensionless Data Analysis, Ph.D. Thesis, Universität Karlsruhe (TH), Germany, 2004.